Specific Binding of Different Vesicle Populations by the Hybridization of Membrane-Anchored DNA†

Paul A. Beales and T. Kyle Vanderlick*

Department of Chemical Engineering, Princeton University, Princeton, New Jersey 08544

Received: July 23, 2007; In Final Form: October 12, 2007

We demonstrate a method of heterogeneous vesicle binding using membrane-anchored, single-stranded DNA that can be used over several orders of magnitude in vesicle size, as demonstrated for large 100 nm vesicles and giant vesicles several microns in diameter. The aggregation behavior is studied for a range of DNA surface concentrations and solution ionic strengths. Three analogous states of aggregation are observed on both vesicle size scales. We explain the existence of these three regimes by a combination of DNA binding favorability, vesicle collision kinetics, and lateral diffusion of the DNA within the fluid membrane. The reversibility of the DNA hybridization allows dissociation of the structures formed and can be achieved either thermally or by a reduction in the ionic strength of the external aqueous environment. Difficulty is found in fully unbinding giant vesicles by thermal dehybridization, possibly frustrated by the attractive van der Waals minimum in the intermembrane potential when brought into close contact by DNA binding. This obstacle can be overcome by the isothermal reduction of the ionic strength of the solution: this reduces the Debye screening length, coupling the effects of DNA dehybridization and intermembrane repulsion due to the increased electrostatic repulsion between the highly charged DNA backbones.

Introduction

Lipid membranes, used by nature as the basis for functional cellular packaging material, are readily created in the laboratory in the form of vesicles, which are deformable, well-sealed, and self-healing. Their robust and bioinspired properties make lipid vesicles ideal for applications and new technologies that require small containers.[1] For example, lipid vesicles could be deployed in microfluidic devices for the controlled confinement, transport, and manipulation of chemical cargo.[2,3] The ability to induce fusion between lipid vesicles where their internal contents become mixed could be used to instigate chemical reactions in small volumes; this has the advantages of rapid and efficient mixing and the use of very small amounts of reagents. The promise and efficiency of such technologies can be enhanced by the development of techniques to control the association and dissociation of different vesicle populations.

A strategy that has been employed for the assembly of binary hard-sphere colloids is DNA-mediated adhesion.[4−7] Single-stranded DNA is covalently conjugated to the surface of the colloidal particles. The colloids then bind specifically to a second population of colloids that express the complementary ssDNA sequence. The high specificity of binding between complementary sequences and the digital nature of DNA base coding enable the programmable assembly of colloidal aggregates. The binding of DNA duplexes is reversible and usually instigated by heating above the melting transition temperature for the DNA sequence. This allows for the reversibility of colloidal aggregation and the annealing of the aggregates formed. DNA binding stability is also affected by other controllable parameters, such as the ionic strength of the solution and the concentration of DNA.[8,9] The prospect exists for having numerous different single-stranded DNA (ssDNA) sequences expressed by different colloid populations to program the assembly of superstructures with high degrees of complexity.[10]

A DNA-mediated approach would be an effective solution to the controllable association of different populations of lipid vesicles. Vesicles are soft, deformable colloids with a fluid interface. This would lead to appreciable differences in the physical processes of assembly of lipid vesicles mediated by DNA. Unlike the hard-sphere colloids, vesicles would be able to deform upon adhesion, and the capacity of the DNA to diffuse about the vesicle surface could result in the DNA localizing in specific regions of the membrane, for instance the binding sites.

The study of interactions between lipid vesicles has received much attention. Aggregation of like vesicles has previously been reported by the addition of streptavidin to solutions containing vesicles with a small proportion of biotin-modified lipid headgroups.[11] Other methods of vesicle homoaggregation by site-specific binding can be found in the literature.[12,13] Heteroaggregation between vesicles containing synthetic amphiphiles with complimentary molecular recognition groups has also been achieved.[14,15] One study synthesized lipids with single DNA bases as functionalized headgroups. When incorporated into different giant vesicles, hemifusion and, in a small number of cases, fusion was observed between vesicles.[16] However, this approach does not allow the programmable assembly of vesicle superstructures, since several DNA bases in sequence would be required for recognition between many vesicle populations.

DNA-modified vesicles have been reported for the anchoring of vesicles to solid substrates[17] and surface-supported membranes.[18,19] However, to the best of our knowledge, this is the first study of vesicle−vesicle interactions mediated by the hybridization between complementary DNA strands. We use ssDNA oligonucleotides with a cholesterol modification on one of the ends (chol-DNA). The free energy difference between cholesterol existing in the aqueous phase or partitioning into a lipid bilayer is estimated to be approximately $23k_BT$.[20] Therefore,

† Part of the "Giacinto Scoles Festschrift".

* Corresponding author. E-mail: vandertk@princeton.edu.

10.1021/jp075792z CCC: $37.00
Published on Web 11/13/2007

the hydrophobic moiety of the cholesterol, a molecule native to biological membranes, buries itself into the hydrophobic core of the lipid bilayer, anchoring the single-stranded DNA to the outer monolayer of the vesicle surface.

Techniques are available to make unilamellar lipid vesicles with diameters ranging over approximately 4 orders of magnitude ($10^{-8}-10^{-4}$ m). This offers a range of membrane surface area (which can act as a 2D solvent for hydrophobic molecules) over 8 orders of magnitude and a 12 order of magnitude variation in encapsulated volume in which hydrophilic species can be contained. The preferred vesicle size range can be selected for the specific application; therefore, it would be desirable to demonstrate that a technique used to produce hierarchical structures of assembled vesicles is applicable over a wide range of vesicle sizes. In this paper, we demonstrate the assembly of vesicles on two length scales: large unilamellar vesicles (LUVs) with an average diameter of ~100 nm and giant unilamellar vesicles (GUVs) with diameters greater than 5 μm.

Methods

Materials. The lipid 1-palmitoyl-2-oleoyl-*sn*-glycero-3-phosphocholine (POPC) was purchased from Avanti Polar Lipids, Inc. (Alabaster, AL). The fluorescent lipids Lissamine rhodamine B 1,2-dihexadecanoyl-*sn*-glycero-3-phosphoethanolamine, triethylammonium salt (Rh-DPPE) and Oregon Green 488 1,2-dihexadecanoyl-*sn*-glycero-3-phosphoethanolamine (Oregon Green DPPE) were purchased from Invitrogen−Molecular Probes. The oligonucleotides with a cholesteryl-TEG modification on the 5′ ends were synthesized and purified by HPLC by Eurogentec North America (San Diego, CA). The oligonucleotide sequences were 5′-ACAGACTACC-3′ (10mer-1), 5′-GGTAGTCTGT-3′ (10mer-2), 5′-ATTGACTT-3′ (8mer-1), and 5′-AAGTCAAT-3′ (8mer-2).

LUVs were prepared by the extrusion method. Approximately 1 mL of 20 mg/mL POPC in chloroform was placed into a glass vial and evaporated under vacuum for at least 4 h to remove all the solvent and leave a lipid film at the bottom of the vial. Two milliliters of 125 mM sodium chloride and 10 mM Hepes buffered to a pH of 7.4 and a measured osmolarity of 260 mOsm was added to the vial. The sample was vortexed, frozen, and then thawed five times before extruding ten times through two Whatman Nucleopore track-etch membranes with pore sizes of 100 nm. Lipid concentrations were measured using a standard phosphate assay.

GUVs were prepared by electroformation. Seventy microliters of 1.0 mM POPC in chloroform plus 1.0 mol % fluorophore (either Rh-DPPE or Oregon Green DPPE) was spread onto two platinum wires in a home-built electroformation chamber and dried under vacuum for at least 4 h. The chamber was filled with a 300 mM sucrose solution (approximately 3 mL) and a 3 V ac electric field applied: 10 Hz for 30 min, 3 Hz for 15 min, 1 Hz for 7 min, and then 0.5 Hz for 7 min. The vesicle solution was then removed from the chamber and stored in a plastic vial.

The concentrations of chol-DNA solutions were calculated from theoretical extinction coefficients by measuring UV adsorption at 260 nm using a Spectronic GENESYS 2 UV−vis spectrophotometer (Thermo Scientific). The desired concentration of chol-DNA was mixed into prepared vesicle solutions. A period of at least 30 min was allowed for the cholesterol anchors to diffuse into the vesicle membranes before experiments began.

Laser Scanning Confocal Microscopy. Images of solutions of GUVs were obtained using the Leica TCS SP5 confocal system. The objective lens used was a Leica 63×/1.3 N.A. Plan Apo DIC Glycerin immersion lens. The Rh-DPPE probe was excited by a DPSS laser at 561 nm and the Oregon Green DPPE probe was excited with the 488 nm line of an argon laser. A single channel heater controller (model TC-324B) was used in conjunction with a DH-40I temperature stage (Warner Instruments) for experiments where the samples were heated. Glass bottom culture dishes (MatTek Corporation, part no. P35G-1.5-20-C) were treated with a 10% bovine serum albumin (Sigma) solution prior to use in order to prevent the vesicles from adhering to the glass coverslip.

Digital Video Imaging. Samples were taped to the inside of the window of a model 281A Isotemp vacuum oven (Fisher Scientific) and imaged using a Panasonic PV-GS250 video camera. Movies were edited using Final Cut Pro 5.0 software (Apple).

Dynamic Light Scattering. Samples of LUVs were studied by dynamic light scattering (DLS) using a Brookhaven Instruments BI-200SM goniometer, an ALV-5000E digital correlator, and a Coherent Compass 315M 100 mW, double-pumped, continuous wave, solid-state NdYAG laser with 532 nm emission wavelength. The goniometer bath temperature was set to 20 °C. The size distribution of vesicle aggregates in the sample was calculated from the apparent diffusion constant obtained from the normalized intensity correlation function at a scattering angle of 90° using a second-order cumulant data analysis. Scattered intensities were collected for between 2 and 5 min per measurement (the exception being the early time aggregation kinetics, where collection times as short as 10 s were used). Repeat measurements were taken to ensure the reproducibility of the apparent size distribution.

Results and Discussion

We will first present data on the binding of LUVs, which, with a mean diameter of 100 nm, are smaller than the diffraction limit of visible light and therefore cannot be directly observed by conventional optical microscopy techniques. The advantage of LUVs is that vesicle populations with a narrow size distribution can be formed and bulk techniques can be used to obtain the ensemble average behavior of the system, yielding data with high statistics. This will be followed by a section on direct observations of the assembly of GUVs using confocal microscopy.

Large Unilamellar Vesicles (LUVs). LUVs prepared by extrusion had an average hydrodynamic radius of around 50 nm, as determined by dynamic light scattering. One milliliter of 1.0 mM POPC LUVs with membrane-bound 10mer-1 chol-DNA (such that there was an average of 155 chol-DNA per vesicle) was added to 1.0 mL of 1.0 mM POPC (with an average of 155 of the complementary 10mer-2 chol-DNA per vesicle). The solution, which was originally clear, noticeably became more turbid over several hours until white, fluffy flocculates dropped out of solution.

The observed aggregation is caused by the hybridization of the two complementary DNA strands anchored to different vesicles, linking the vesicles by a double-stranded DNA duplex. No aggregation was seen in samples of POPC vesicles alone and in samples of POPC vesicles containing only one species of chol-DNA. This was confirmed by DLS: no change in the size distribution of these vesicle solutions was observed over several days. This suggests that no significant nonspecific aggregation occurs between POPC vesicles or POPC vesicles decorated with noncomplementary chol-DNA, since aggregation was only observed for samples containing two vesicle populations with complementary ssDNA sequences anchored to them.

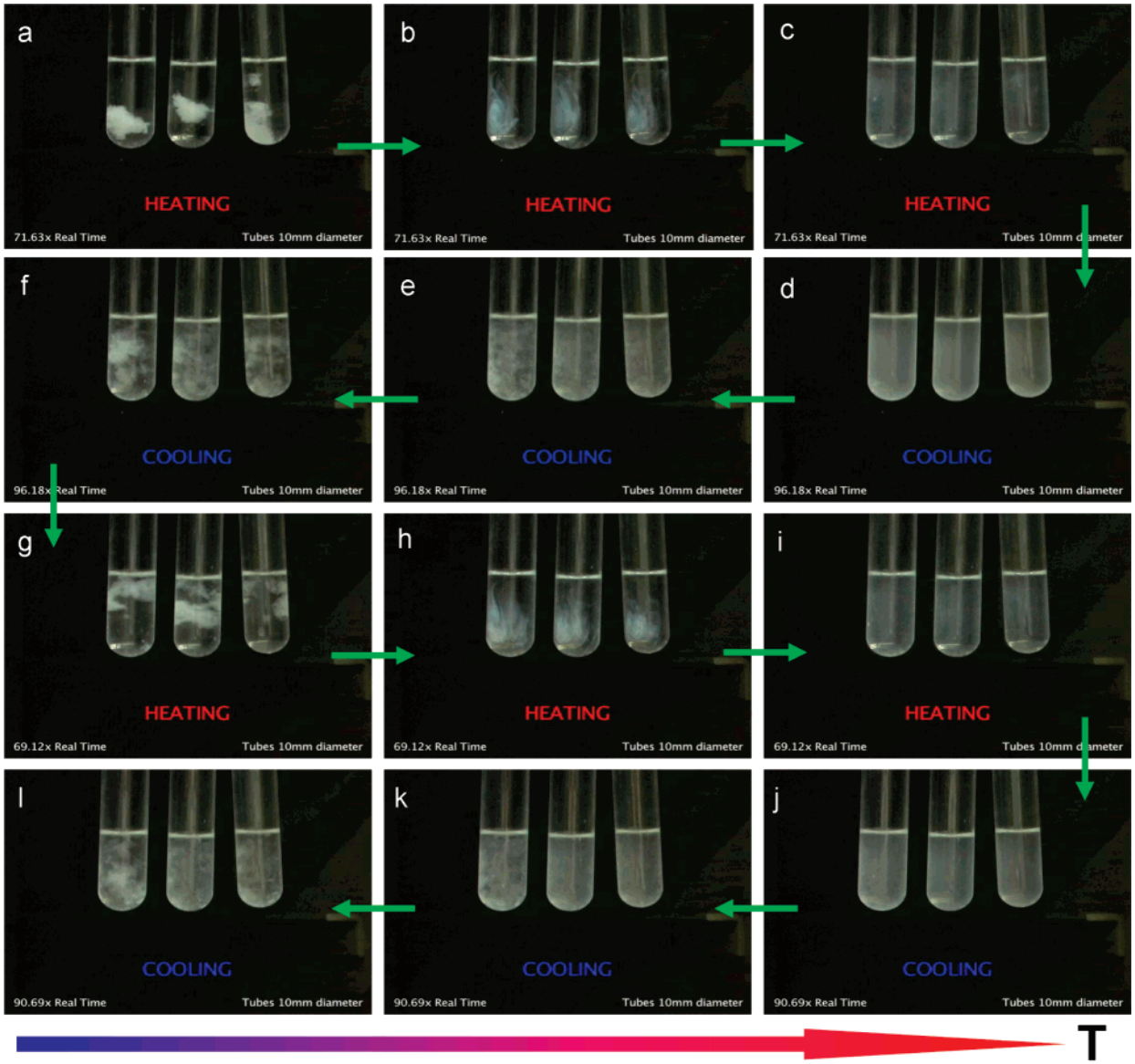

Figure 1. Screenshots, taken from the movie in the Supporting Information, demonstrate thermally driven unbinding and rebinding of vesicle assemblies. Vesicles contain an average of 155 chol-DNA per vesicle. (a−c) Heating disperses the vesicle conglomerates, leaving a clear, homogeneous solution; (d−f) on cooling, the turbidity of the solutions increases as the vesicles rebind, with the aggregates increasing in size until flocculates become visible; (g−i) reheating again causes the vesicle assemblies to disperse; (j−l) rebinding is again observed on cooling. Tube diameters are 10 mm. Temperature increases from left to right in the schematic.

Short DNA duplexes are known to unbind above a melting transition temperature. Flocculated samples with 155 chol-DNA per vesicle were placed into a glass-fronted oven and heated. Samples were observed with a video camera. The flocculates were seen to disperse back into solution, leaving a clear homogeneous sample. On cooling, the solution could be seen to increase in turbidity and the fluffy, white flocculates eventually reappeared in the sample. Unbinding and rebinding of the vesicles were successfully repeated five times for the same samples with no indication that further cycles might be unsuccessful (see the movie in the Supporting Information). Screenshots from this movie demonstrating two unbinding-rebinding cycles are illustrated in Figure 1.

Vesicle unbinding was also achieved in the light-scattering apparatus. When the goniometer bath was heated to 60 °C, samples with 155 chol-DNA per vesicle were observed to return to an average size and polydispersity comparable to that of the single POPC vesicles. This implies that the vesicles were fully unbound from each other due to the melting of the DNA duplex. It can also be deduced that no fusion had occurred between vesicles while bound together by the DNA, since vesicle fusion is irreversible and would have resulted in the measurement of a larger vesicle size distribution.

The early stages of aggregate growth kinetics were studied for several chol-DNA per vesicle ratios for the two complementary 10-mer chol-DNAs. The average hydrodynamic radius (R_h) of aggregates in solution was measured by DLS as a function of time (t) after initial mixing of the two vesicle populations. Figure 2A shows the dimensionless size of the aggregates (R_h/R_0) as a function of time, where R_0 is the average hydrodynamic radius of the monomeric POPC vesicles (i.e., the average size of aggregates at $t = 0$). Three regimes of aggregation behavior were observed. At an average of 2.5 ssDNA per vesicle, no significant aggregation was observed over several days: a measured average value of $R_h/R_0 = 1.027$. At an average of 19 chol-DNA per vesicle, stable aggregate sizes averaging $R_h/R_0 = 1.43$ were measured within several minutes: these aggregate sizes were stable over a few days. At

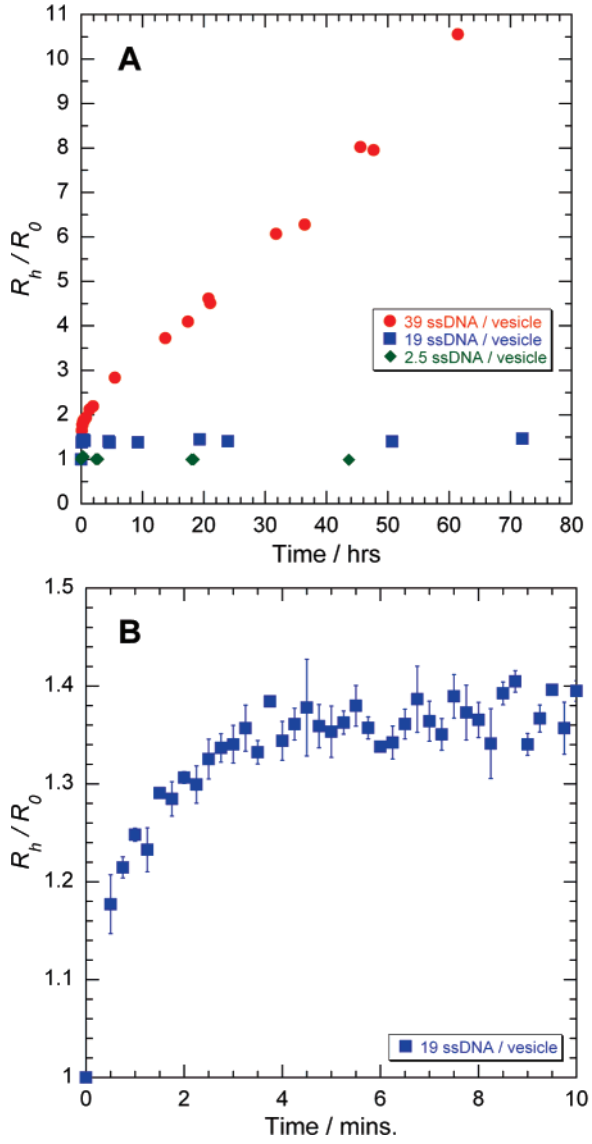

Figure 2. (A) Aggregation kinetics of POPC LUVs decorated with different amounts of membrane-anchored ssDNA: (◆) 2.5 ssDNA per vesicle, (■) 19 ssDNA per vesicle, and (●) 39 ssDNA per vesicle. The normalized aggregate size (R_h/R_0), where R_h is the measured hydrodynamic radius and R_0 is the measured hydrodynamic radius of the monomeric POPC vesicles, is plotted against time in hours. (B) The initial stages of the aggregation kinetics for samples with 19 ssDNA per vesicle. The normalized aggregate size (R_h/R_0) is plotted against time in minutes. All samples are measured at 20 °C.

an average of 39 chol-DNA per vesicle, continuous aggregation was observed. Aggregation continued until visible white flocculates dropped out of solution after several days, as was previously observed for the 155 chol-DNA per vesicle samples.

It is interesting to note that an average of several (a lower bound of greater than 2.5) ssDNA per vesicle is necessary before significant aggregation between vesicles is detected. This suggests that a single DNA bond between vesicles is not sufficient to maintain vesicle adhesion and that more DNA must diffuse into the binding site and hybridize with its complement such that multiple DNA bonds reinforce and maintain the adhesion between vesicles. It should also be noted that the binding stability, as measured by the melting temperature, of a DNA duplex is dependent on the concentration of DNA in solution.[8,9] Therefore, the effective local surface concentration of ssDNA on the surface of the vesicles must be high enough for duplex formation to be stable. Increasing the number of ssDNA per vesicle will increase the effective local concentration that the DNA experiences and hence will increase its binding affinity with its complement.

For the case of stable aggregates, DNA must localize in the binding sites such that there is not a sufficient excess of unbound ssDNA on the surface of the aggregate to stably bind to further vesicles in solution. This would seem reasonable, since we can estimate the time scale needed for ssDNA to diffuse into the binding site by estimating that the membrane-bound chol-DNA has a similar lateral diffusion constant to that of lipids in a fluid bilayer: $D_{DNA} \approx 5 \times 10^{-8}$ cm^2 s^{-1}.[21] The time (t_{DNA}) for the chol-DNA to diffuse the circumference of the 100 nm diameter vesicle, an estimate of the relevant length scale (x), would be $t_{DNA} = \langle x^2 \rangle / 4D_{DNA} \approx 5$ ms. The time between collisions can be estimated using Smoluchowski's coagulation theory, where the half-time of rapid coagulation, $t_{1/2} = 3\eta/4k_BTn_0$.[22] Here η is the dynamic viscosity of the solution (1.002×10^{-3} Pa s), k_B is Boltzmann's constant, T is the temperature (293 K), and n_0 is the initial concentration of vesicles in solution ($\approx 6 \times 10^{18}$ m^{-3} for a 1.0 mM solution of 100 nm diameter vesicles, assuming an area per lipid headgroup of ~69 Å^2 [23]). Therefore, $t_{1/2} \approx 31$ ms. However, this half-time assumes that every collision results in coagulation. It can be seen from the initial kinetics of aggregation for 19 ssDNA per vesicle in Figure 2B that the time scale for effective collisions (t_{eff}) that result in vesicle binding for these small aggregates is on the order of minutes, so the binding probability upon collision is very small ($\leq 10^{-3}$). Therefore, $t_{DNA} \ll t_{eff}$; hence, DNA has time to accumulate in the binding site before the next potentially effective binding collision with another vesicle or vesicle aggregate.

At higher DNA per lipid, as we see for 39 ssDNA per vesicle, once DNA has saturated in the binding site between vesicles, there must always be a sufficient excess of ssDNA on the surface of the aggregate for it to bind with further vesicles or vesicle aggregates until the sample becomes flocculated. A more in-depth analysis of the binding kinetics between vesicles mediated by DNA hybridization will be the subject of future work from our laboratory.

Giant Unilamellar Vesicles (GUVs). DNA-mediated association of giant vesicles was investigated by confocal microscopy. GUVs with the complementary ssDNA anchored to their membranes were mixed at least 24 h before observation. Samples were observed under a confocal microscope in order to look for binding between vesicles. The concentration of chol-DNA per lipid and sodium chloride concentration added to the external solution after vesicle formation were varied. Vesicles could be determined to be bound together by observing their diffusive motion. Adjacent vesicles that were observed to diffuse collectively were deemed to be bound together. Control experiments of vesicles with only one ssDNA sequence (i.e., 10mer-1 or 10mer-2) anchored to the vesicles in solution and vesicles with no ssDNA anchored to their membranes with and without 55 mM sodium chloride in the external solution were carried out: no aggregation was observed for these cases (data not shown). Therefore, we conclude that vesicle binding is due to the specific interaction between complementary ssDNA anchored to the vesicle membranes.

Different states of aggregation were observed for vesicles with the complementary 10mer-1 and 10mer-2 bound to their membranes: no binding, small clusters coexisting with monomeric vesicles, and large clusters with very few monomers observed (Figure 3). In Figure 3A−C, corresponding to no

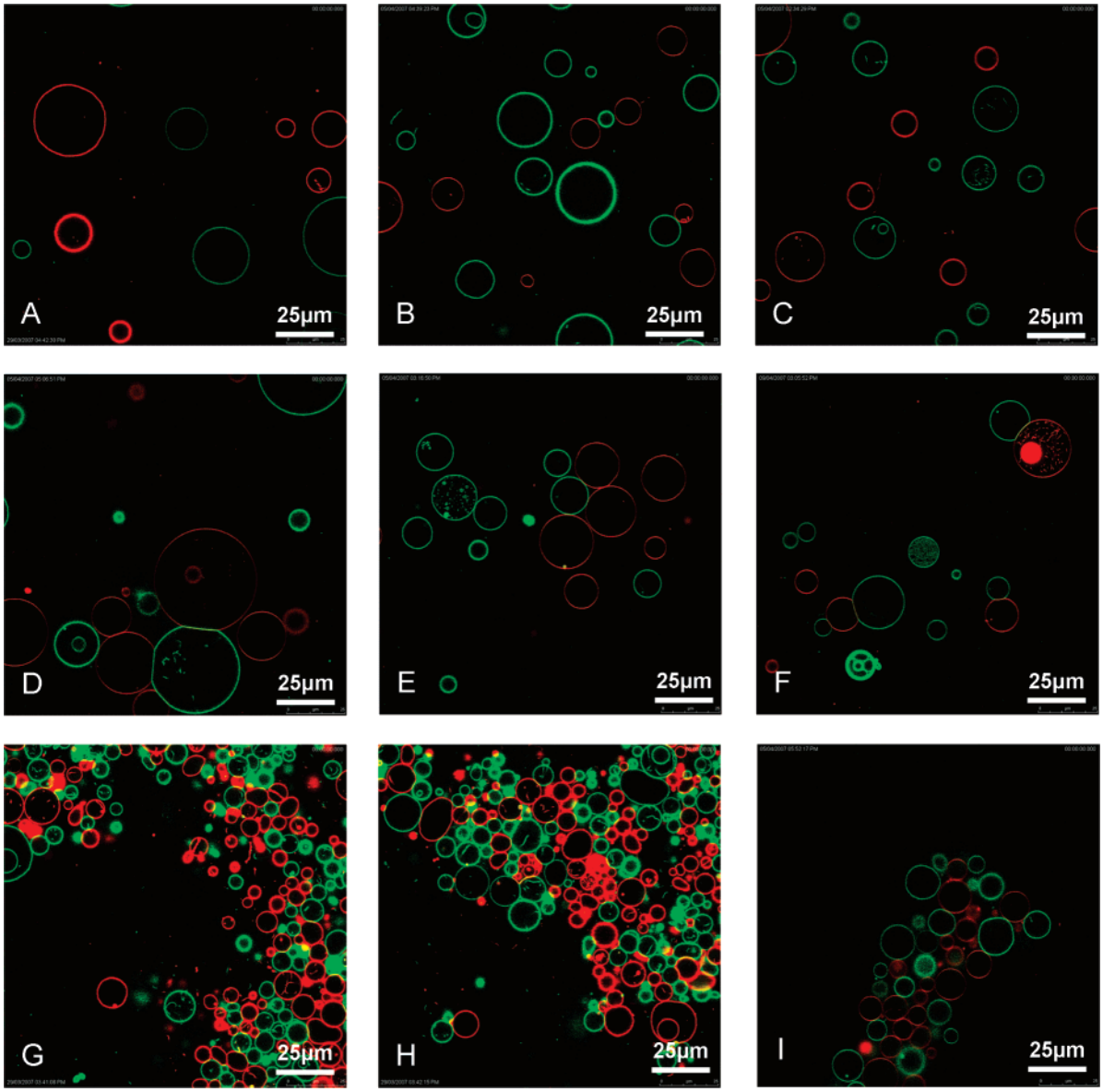

Figure 3. Representative images of the three states observed upon varying 10mer ssDNA per lipid and sodium ion concentration: (A−C) no discernible aggregation, (D−F) small aggregates coexisting with vesicle monomers, (G−I) large aggregates. (A) 5.0×10^{-3} ssDNA/lipid, 7.8 mM Na^+; (B) 2.5×10^{-3} ssDNA/lipid, 15 mM Na^+; (C) 1.3×10^{-3} ssDNA/lipid, 15 mM Na^+; (D) 2.5×10^{-3} ssDNA/lipid, 38 mM Na^+; (E) 1.3×10^{-3} ssDNA/lipid, 38 mM Na^+; (F) 5.0×10^{-3} ssDNA/lipid, 38 mM Na^+; (G) 5.0×10^{-3} ssDNA/lipid, 55 mM Na^+; (H) 5.0×10^{-3} ssDNA/lipid, 55 mM Na^+; (I) 1.3×10^{-3} ssDNA/lipid, 47 mM Na^+. Chol-DNA 10mer-1 is bound to the green vesicles and 10mer-2 is bound to the red vesicles. Scale bars represent 25 μm.

aggregation, all vesicles that appear to be in close spatial proximity were observed to diffuse away from each other over time and hence were not considered as aggregates. Figure 3D−F shows small vesicle aggregates, which diffuse collectively, coexisting with unbound vesicle monomers. Large vesicle aggregates can be seen in Figure 3G−I; very few unbound vesicles could be found in these samples.

A map of our observations upon varying ssDNA per lipid and sodium ion concentration is shown in Figure 4. Vesicle clustering is observed to increase upon increasing ssDNA per lipid and increasing the salt concentration. No vesicle binding was observed without the addition of sodium chloride. This is due to the high negative charge of the sugar−phosphate DNA backbones, which needs to be screened by positive (e.g., sodium) ions for hydrogen bonding between the complementary bases of the DNA to be energetically favorable. This is in qualitative agreement with experiments that show that an increase in sodium ion concentration increases the thermal stability of the double-stranded duplex formed by short, complementary ssDNA oligomers.[24] The duplex thermal stability is also predicted to increase logarithmically with increasing oligo concentration.[8,9]

Three states of aggregation were reported for the LUVs (no aggregation, stable aggregates, and continual growth to flocculation) and it is reasonable to assume that these are the analogous states to those we observe for the GUVs, even though different regions of phase space are explored. All LUV experiments were conducted at $[Na^+] = 125$ mM, and the DNA coverage from 2.5 to 39 DNA per vesicle corresponds to surface concentrations in the range from 2.5×10^{-5} to 4.0×10^{-4} DNA per lipid. The observations with GUVs were conducted at lower ionic strengths (7.8 mM $\leq [Na^+] \leq$ 82 mM) and higher surface concentrations (from 5×10^{-4} to 5×10^{-3} DNA per lipid). In spite of these slight differences in ionic strength and DNA surface concentrations, both systems conserve three aggregation regimes, even though vesicle sizes range over 2 orders of magnitude. Size, however, may not be irrelevant, as the

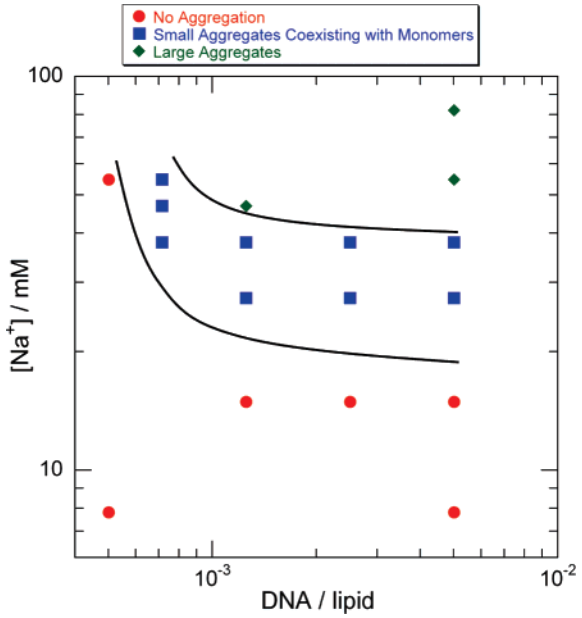

Figure 4. Phase diagram mapping the observed states upon varying 10mer ssDNA per lipid and sodium ion concentration for GUVs at 22 °C: ● represents no discernible aggregation; ■ represents small aggregates coexisting with vesicle monomers; ◆ represents large aggregates and negligible vesicle monomers. Approximate phase boundaries are drawn to guide the eye.

underlying physical processes of vesicle binding may be controlled by the numbers of DNA per vesicle and not just by surface concentration; this is expected for the LUVs where those numbers approach the order of unity.

In contrast with the LUVs, GUVs are each decorated with up to 10^7 ssDNA. Therefore, the regime of no aggregation must originate from either the conditions (temperature, ionic strength, and local surface concentration of ssDNA) being unfavorable for duplex formation or the strength of adhesion between vesicles when a single DNA bond forms being too weak to maintain close contact for sufficient time for further ssDNA to diffuse into the binding site and form further DNA bonds. It can be seen in Figure 3D−F that, for the small aggregates regime, large (several microns in diameter) osculating areas form between adhering vesicles. This growth of the adhesion plaque is made possible by the deformability of the membrane and the fluid nature of the lipid bilayer allowing DNA to diffuse into and enhance the binding site. The local concentration enhancement of DNA into the binding site would deplete the rest of the membrane of ssDNA, possibly to the point where the surface concentration of ssDNA became too low for adhesion to further vesicles to be favorable, limiting the size of aggregates that form to small clusters of vesicles. As the salt concentration and/or the surface concentration of ssDNA is further increased, a regime will be reached where, once the adhesion plaque is saturated with DNA, sufficient ssDNA will always remain in the unbound membrane area such that adhesion to further vesicles is always favorable, causing large-scale aggregates to form, as seen in Figure 3G−I.

Comparisons can be made between our system and the more extensively studied DNA-grafted hard-sphere colloids. We note that the observed phases in Figure 3 are analogous to those previously reported by Biancaniello et al.[4] However, a direct quantitative comparison cannot be drawn between our phase diagram and that of Biancaniello et al.[4] for several reasons: (i) We used surface-anchored ssDNAs of a different sequence and length and hence they have a different binding affinity. (ii) Biancaniello et al. changed the number of ssDNAs anchored to their colloids by absorbing a mixture of complementary and noncomplementary (inert) ssDNAs to the target colloids, thus keeping the total DNA surface density fixed. In our case the surface density varies since no inert DNA is used. (iii) The ssDNA has fixed anchor points on the surface of the polystyrene colloids used by Biancaniello et al., in contrast to the chol-DNA, which is anchored to the fluid lipid bilayer by hydrophobic forces and hence is free to diffuse about the surface and, for instance, localize in the binding sites, resulting in enhanced surface concentrations of ssDNA in these adhesive plaques. (iv) The hard-sphere polystyrene colloids are not visibly deformed in the adhesion process compared to the lipid vesicles, whose soft, flexible membranes can be deformed by the work of adhesion, providing visibly flattened and extended osculating regions between adhering vesicles that further enhance the number of DNA linkages in each binding site.

The integrity of the vesicles was not compromised by the assembly technique: no vesicle fusion or intermembrane mixing resulted from the DNA-mediated association. From the images in Figure 3, it can be seen that the Rh-DPPE (red) and Oregon Green DPPE (green) dyes do not transfer between vesicles in a given conglomerate: this implies that there is no lipid mixing between vesicles. Therefore, the membrane components and the internal contents of the vesicles remain isolated, despite being bound in close spatial proximity, as was inferred from our results on binding and unbinding of LUVs.

The fidelity of red to green vesicle binding in this system is not flawless. Looking at Figure 3 as a whole, red vesicles sometimes appear to be bound to other red vesicles, and similarly, there appears to be some homobinding between green vesicles. It is worth bearing in mind that these images are thin, two-dimensional sections through three-dimensional vesicle aggregates and therefore do not reveal any vesicles that are bound above and below the image plane. Many cases of apparent homobinding can be explained by the presence of one of more vesicles of the opposite population out of the image plane binding these vesicles into the conglomerate. However, we do recognize that some binding between like vesicles does also occur in these samples. Since we observed no significant nonspecific binding in our control experiments, we conclude that this is due to some exchange of chol-DNAs between the vesicles in solution. This may occur by a couple of different mechanisms. First, when vesicles are in close spatial proximity, the aqueous gap between adjacent membranes may become small enough that the energy barrier to the cholesterol moiety flipping between membranes becomes small enough that the probability of chol-DNA exchange becomes significant over our experimental time scale. Second, there could be a small proportion of chol-DNA that remains soluble in the aqueous phase and a dynamic equilibrium between membrane-bound chol-DNA and soluble chol-DNA exists. These possible mechanisms are, of course, not mutually exclusive; hence, both could contribute to some exchange of chol-DNA between vesicle populations.

The exchange of chol-DNAs between vesicle populations in the GUV samples might be exacerbated by the presence of sucrose in the aqueous solution compared to the experiments with LUVs in the previous section, which were carried out in a buffered sodium chloride solution. This is because cyclodextrins, cyclic molecules made of sugars, are known to remove cholesterol from cell membranes.[25] Since more than a quarter of the molecular surface area of sucrose is nonpolar,[26] sucrose molecules may preferentially order around the cholesterol moiety

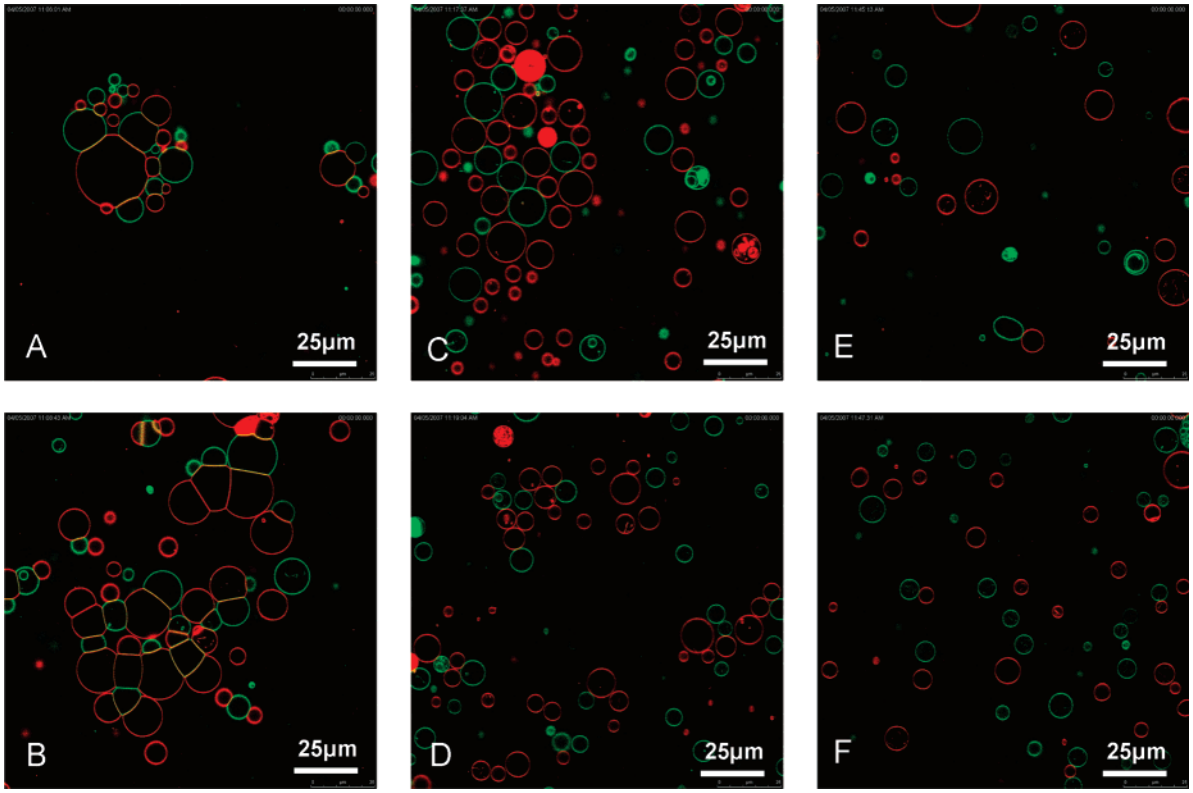

Figure 5. Unbinding of vesicle superstructures by reduction of the ionic strength of the external aqueous phase. Sample contains 5.0×10^{-3} 8mer ssDNA/lipid. (A, B) 98 mM Na^+: vesicles are strongly adhering; 3 mL of 320 mM glucose solution is added, reducing the sodium ion concentration to 6.2 mM. (C, D) After approximately 5 min, weaker vesicle binding is observed, as seen by the reduction in contact angle and osculating areas. (E, F) After approximately 30 min, vesicles are unbound and diffusing as monomers. Scale bars represent 25 μm.

of the chol-DNA to reduce the free energy difference between being anchored to the membrane and being soluble in the aqueous phase. Apart from this subtle effect, we do not expect the presence of sucrose to have any undesirable influences on system behavior (although we note that sucrose serves to reduce slightly the melting temperature of oligonucleotide duplexes but also to increase the enthalpy of unbinding[27]).

Exchange of membrane-bound DNAs between vesicle populations could be reduced by increasing the strength of the binding to the lipid bilayer. One study has linked oligonucleotides with a disulfide group on one end to the lipid DPPE, which is modified to have a reactive headgroup.[19] Another possible way to increase the strength of the membrane anchorage is to bind the ssDNA to the membrane via two cholesterol moieties.[28] This is achieved by having two varieties of chol-DNAs in each vesicle population. One chol-DNA is complementary to the lower part of the base sequence of the other chol-DNA, leaving the upper portion of the base sequence of this second chol-DNA as a "sticky" section that could bind to a complementary sequence that might be displayed by a second vesicle population.

Regardless of which vesicles are bound to each other, the binding between GUVs is solely due to the DNA hybridization interaction. Therefore, the interaction should be reversible, resulting in the disassembly of bound vesicles. One possible avenue to achieve vesicle unbinding is by the reduction of the ionic strength of the external solution, since DNA hybridization requires a sufficient concentration of counterions to screen the electrostatic repulsion of their charged backbones. Figure 5A,B shows vesicles bound together by the two complementary 8-mer chol-DNAs. Binding can be seen to be strong, since the vesicles are deformed from their natural spherical shape, due to large osculating areas caused by the binding between membranes. An iso-osmolar glucose solution is added to the sample to dilute

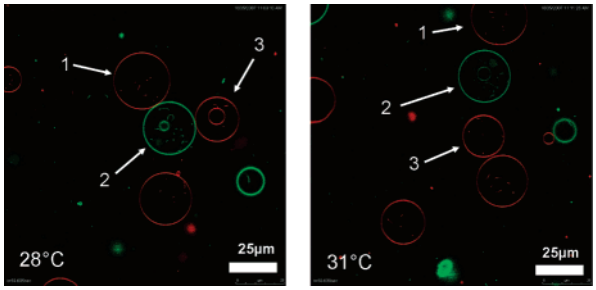

Figure 6. Thermal unbinding of DNA-bound vesicles. Vesicles contain 1.3×10^{-3} 8mer ssDNA/lipid in an external solution with a sodium ion concentration of 55 mM. 8mer-1 is bound to green vesicles and 8mer-2 is bound to red vesicles. The numbered vesicles in the weakly bound assembly at 28 °C (left) correspond to the vesicles in the unbound state at 31 °C (right). Scale bars represent 25 μm.

the sodium counterions and thereby reduce the electrostatic screening between the DNA backbones. Within 5 min, reduced adhesion between the vesicles could be seen due to a decrease in the vesicle contact angle and reduction in osculating areas, resulting in a return to their native spherical morphology (Figure 5C,D). However, the vesicles could still be seen to diffuse collectively in their conglomerates. After approximately 30 min, the vesicle assemblies had completely dissociated, with vesicles observed to be diffusing monomerically (Figure 5E,F).

Evidence of vesicle unbinding was also observed on increasing temperature. Figure 6 shows the unbinding of a small conglomerate bound together by the 8mer-1 and 8mer-2 chol-DNAs. The vesicles can be seen to be weakly bound at 28 °C, since the vesicles have maintained their spherical shape in the binding interaction. When the temperature is increased to 31 °C, the vesicles are unbound and have drifted apart. However, full thermal unbinding of all vesicles was not observed in any

samples. This may be for several reasons. First, the temperature range of the heating stage may not have been high enough for the complete melting of all DNA duplexes. Samples could only be heated to slightly above 40 °C. Second, a strong van der Waals minimum in the interaction potential between the giant vesicles could be frustrating vesicle dissociation. The reversibility of binding of micron-sized, hard-sphere colloids linked by hybridized DNA strands has proven problematic. A deep, attractive van der Waals minimum in the interaction potential at short-range causes irreversible aggregation between colloids of this size (a problem that does not occur for nanoscale colloids). This was solved by sterically stabilizing the colloids with grafted polymers such that the interaction between colloids was repulsive upon DNA dehybridization.[7]

GUVs composed of neutral lipids are known to adhere to each other due to the van der Waals interaction when forced into contact such that there exists a large contact area between them.[29] However, additional short-range, repulsive interactions are present between lipid vesicles that do not factor in between hard-sphere colloids. These are the hydration force, which is monotonically repulsive between fluid membranes (hydration forces oscillate between attractive and repulsive between hard, hydrophilic surfaces), and steric repulsion due to the thermal fluctuations of the fluid membrane.[30] These repulsive interactions can decrease the attraction between vesicles by up to 3 orders of magnitude.[30]

Sterically stabilizing the GUVs with, for instance, a lipid-anchored PEG is unlikely to have a similar benefit, as seen with the hard-sphere colloids in aiding the unbinding of vesicles upon DNA dehybridization.[7] This is due to the fluid nature of the lipid bilayer, which would result in these polymer stabilizers diffusing out of and being sterically excluded from any adhesive contacts between vesicles. One solution to overcome any nonspecific attraction between vesicles would be to add a small amount of charged lipid to the vesicles. It has been shown that nonspecific vesicle−vesicle attraction disappears at charge densities as low as ~0.07 charge/lipid.[29] Indeed, our ability to unbind GUVs by reducing the ionic strength of the solution, and thereby reduce the Debye screening length (κ^{-1}), suggests that an increase in electrostatic repulsion between the highly charged sugar−phosphate backbones of the vesicle-anchored ssDNAs not only results in the dehybridization of the DNA duplexes but also provides the necessary electrostatic repulsion between vesicles to cause the dissociation of vesicle aggregates. Explicitly, for monovalent ions such as sodium chloride, the Debye screening length at 25 °C can be calculated as $\kappa^{-1} = 0.304/[\mathrm{NaCl}]^{1/2}$ nm.[31] Therefore, a reduction in the sodium ion concentration from 98 to 6.2 mM, as is shown in Figure 5, corresponds to approximately a 4-fold increase in κ^{-1} from 0.97 to 3.9 nm. This is significant on the scale of the intermembrane separation of bound vesicles, which can be estimated as the length of the double-stranded 8mer DNA bond. The length per base pair of double-stranded DNA has been measured to be approximately 0.34 nm.[32] Therefore, the intermembrane separation (D) upon binding is approximately 2.7 nm, within the range of the increase in the screening length of electrostatic interactions. The electrostatic potential (ψ) decays exponentially with separation (z) from a surface and is given by the Debye−Hückel theory to be $\psi = \psi_0 e^{-\kappa z}$, where ψ_0 is the potential at the surface. Therefore, by this theory, this 4-fold increase in κ^{-1} results in approximately an 8-fold increase in electrostatic repulsion at the intermembrane separation ($z = D$).

Full thermal dissociation was achieved in the case of LUVs, as discussed in the previous section. The van der Waals attraction is not as prevalent for vesicles of these smaller length scales. Therefore, it can be seen that vesicle size is one of the many parameters that can be used to tune the interactions between the vesicles in these systems. The many variables available to regulate the association and dissociation of the vesicle assemblies, where here we have discussed vesicle size, temperature, ionic strength, and DNA surface density, should lead to a technology for the controllable formation of complex, structured vesicle assemblies.

Summary

We have demonstrated the use of complementary strands of ssDNA anchored to the external monolayer of lipid vesicles by a cholesterol moiety as a technique to bind together different populations of vesicles. Binding can be achieved with vesicles over several length scales, as we have demonstrated here with LUVs and GUVs. The vesicle binding is also reversible, either by thermally unbinding or by decreasing the ionic strength of the exterior solution to cause the DNA duplex to dissociate. The digital nature of the DNA base coding and high specificity of binding of complementary oligomers offer the future prospect of programming the in-solution assembly of sophisticated higher-order vesicle superstructures composed of many different vesicle types with several different ssDNA sequences anchored to their membranes. These sequences act as biomolecular combination locks, binding only to vesicles displaying the complementary sequence.

Acknowledgment. With great joy we dedicate this paper to Giacinto Scoles, in honor of his passion for science and his enthusiasm for collaboration. We acknowledge Joe Goodhouse for technical assistance and support during the confocal microscopy. We also thank Jan Vermant for invaluable discussions about dynamic light scattering.

Supporting Information Available: Movie of the thermal unbinding and rebinding of samples of LUVs. This information is available free of charge via the Internet at http://pubs.acs.org.

References and Notes

(1) Zasadzinski, J. A.; Kisak, E.; Evans, C. *Curr. Opin. Colloid Interface Sci.* **2001**, *6*, 85.
(2) Hong, J. W.; Quake, S. R. *Nat. Biotechnol.* **2003**, *21*, 1179.
(3) Tresset, G.; Iliescu, C. *Appl. Phys. Lett.* **2007**, *90*.
(4) Biancaniello, P. L.; Crocker, J. C.; Hammer, D. A.; Milam, V. T. *Langmuir* **2007**, *23*, 2688.
(5) Biancaniello, P. L.; Kim, A. J.; Crocker, J. C. *Phys. Rev. Lett.* **2005**, *94*.
(6) Mirkin, C. A.; Letsinger, R. L.; Mucic, R. C.; Storhoff, J. J. *Nature* **1996**, *382*, 607.
(7) Valignat, M. P.; Theodoly, O.; Crocker, J. C.; Russel, W. B.; Chaikin, P. M. *Proc. Natl. Acad. Sci. U.S.A.* **2005**, *102*, 4225.
(8) Owczarzy, R.; Vallone, P. M.; Gallo, F. J.; Paner, T. M.; Lane, M. J.; Benight, A. S. *Biopolymers* **1997**, *44*, 217.
(9) SantaLucia, J. *Proc. Natl. Acad. Sci. U.S.A.* **1998**, *95*, 1460.
(10) Licata, N. A.; Tkachenko, A. V. *Phys. Rev. E* **2006**, *74*.
(11) Chiruvolu, S.; Walker, S.; Israelachvili, J.; Schmitt, F. J.; Leckband, D.; Zasadzinski, J. A. *Science* **1994**, *264*, 1753.
(12) Menger, F. M.; Zhang, H. L. *J. Am. Chem. Soc.* **2006**, *128*, 1414.
(13) Wang, C. Z.; Wang, S. Z.; Huang, J. B.; Li, Z. C.; Gao, Q.; Zhu, B. Y. *Langmuir* **2003**, *19*, 7676.
(14) Mart, R. J.; Liem, K. P.; Wang, X.; Webb, S. J. *J. Am. Chem. Soc.* **2006**, *128*, 14462.
(15) Paleos, C. M.; Tsiourvas, D. *Colloid Chem. Ii* **2003**, *227*, 1.
(16) Heuvingh, J.; Pincet, F.; Cribier, S. *Eur. Phys. J. E* **2004**, *14*, 269.
(17) Svedhem, S.; Pfeiffer, I.; Larsson, C.; Wingren, C.; Borrebaeck, C.; Hook, F. *Chembiochem* **2003**, *4*, 339.
(18) Benkoski, J. J.; Hook, F. *J. Phys. Chem. B* **2005**, *109*, 9773.
(19) Yoshina-Ishii, C.; Boxer, S. G. *J. Am. Chem. Soc.* **2003**, *125*, 3696.
(20) Kessel, A.; Ben-Tal, N.; May, S. *Biophys. J.* **2001**, *81*, 643.

(21) Vaz, W. L. C.; Goodsaidzalduondo, F.; Jacobson, K. *FEBS Lett.* **1984**, *174*, 199.
(22) Norde, W. *Colloids and Interfaces in Life Sciences*; Marcel Dekker, Inc.: New York, 2003.
(23) Nagle, J. F.; Tristram-Nagle, S. *Biochim. Biophys. Acta*—Rev. Biomembr. **2000**, *1469*, 159.
(24) Owczarzy, R.; You, Y.; Moreira, B. G.; Manthey, J. A.; Huang, L. Y.; Behlke, M. A.; Walder, J. A. *Biochemistry* **2004**, *43*, 3537.
(25) Zidovetzki, R.; Levitan, I. *Biochim. Biophys. Acta* **2007**, *1768*, 1311.
(26) Street, T. O.; Bolen, D. W.; Rose, G. D. *Proc. Natl. Acad. Sci. U.S.A.* **2006**, *103*, 13997.
(27) Spink, C. H.; Garbett, N.; Chaires, J. B. *Biophys. Chem.* **2007**, *126*, 176.
(28) Pfeiffer, I.; Hook, F. *Anal. Chem.* **2006**, *78*, 7493.
(29) Evans, E. *Langmuir* **1991**, *7*, 1900.
(30) Leckband, D.; Israelachvili, J. *Q. Rev. Biophys.* **2001**, *34*, 105.
(31) Israelachvili, J. *Intermolecular & Surface Forces*, 2nd ed.; Academic Press Inc.: San Diego, CA, 1991.
(32) Marko, J. F.; Siggia, E. D. *Macromolecules* **1995**, *28*, 8759.